Electronic Supplementary Information

Deprotonation-Triggered Ultra-large Stokes Shift of Aqueous NIR-Emissive Hydroxylstryryl-Pyridinium Derivatives

Xiaolong Lu[a,b,c], Liyu Xiong[b,c], Zhihan Zhang[b,c], Haolong Yang[b,c], Enmin Li[d,e,f]* and Hefeng Zhang[b,c]*

a Marine Science Institute, College of Science, Shantou University, Shantou 515063, China
b Key Laboratory for Preparation and Application of Ordered Structural Materials of Guangdong Province, Department of Chemistry, College of Chemistry and Chemical Engineering, Shantou University, Shantou 515063, China
c GuangDong Engineering Technology Research Center of Advanced Polymer Synthesis, College of Chemistry and Chemical Engineering, Shantou University, Shantou 515063, China
d The Key Laboratory of Molecular Biology for High Cancer Incidence Coastal Chaoshan Area, Department of Biochemistry and Molecular Biology, Shantou University Medical College, Shantou 515041, Guangdong, China
e The Laboratory for Cancer Molecular Biology, Shantou Academy Medical Sciences, Shantou 515041, China
f Chaoshan Branch of State Key Laboratory for Esophageal Cancer Prevention and Treatment, Shantou 515063, China

E-mail: (hfzhang@stu.edu.cn, nmli@stu.edu.cn)

1 Experimental method

Materials and Instruments

All materials used in the experiment were purchased from commercial suppliers and used directly without further purification. UV-vis spectra were recorded on UV-Vis-NIR Spectrophotometer (Shanghai, China, UNICO, UV-4802S). Fluorescent spectra were recorded on Steady-state Transient Photoluminescence Spectrometer. Proton and carbon nuclear magnetic resonance spectra (^{1}H NMR and ^{13}C NMR) were recorded on Bruker AVANCE-400 MHz NMR and 100 MHz NMR spectrometer, respectively, with TMS as an internal reference. Mass spectra were measured by High-Resolution Mass Spectrometry (HRMS) (Orbitrap Exploris 120, Thermo Fisher Scientific, US). Absolute photoluminescence quantum yields (QY) of dyes were measured by using the integrating sphere method on spectrometer C11347. The reaction progress was

monitored by thin chromatography (TLC) on silica gel plates. The crude products were purified by flash column chromatography.

2. Supplementary tables and figures

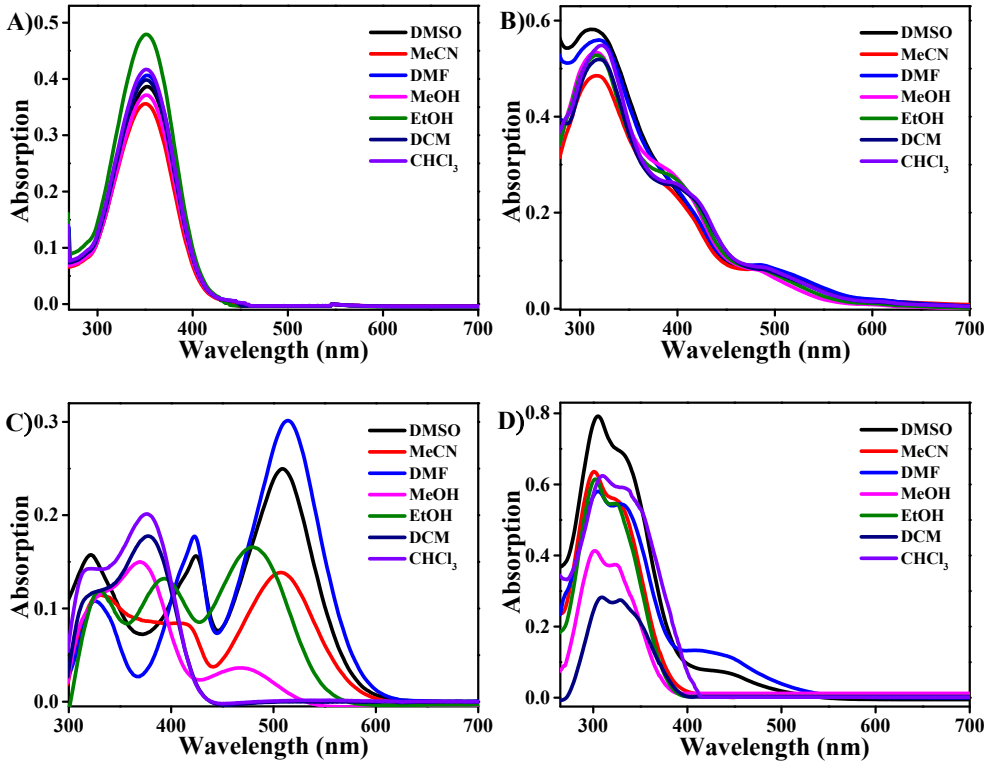

Figure S1. The UV-Vis absorption spectra of SP-OH dyes in different solvents (c = 10^{-5} mol/L).

A) SP-2-NO_2-Py, B) SP-2-NO_2-5-OMe-Py, C) SP-5-NO_2-2-OH-Py, D) SP-2-NO_2-5-OH-Py

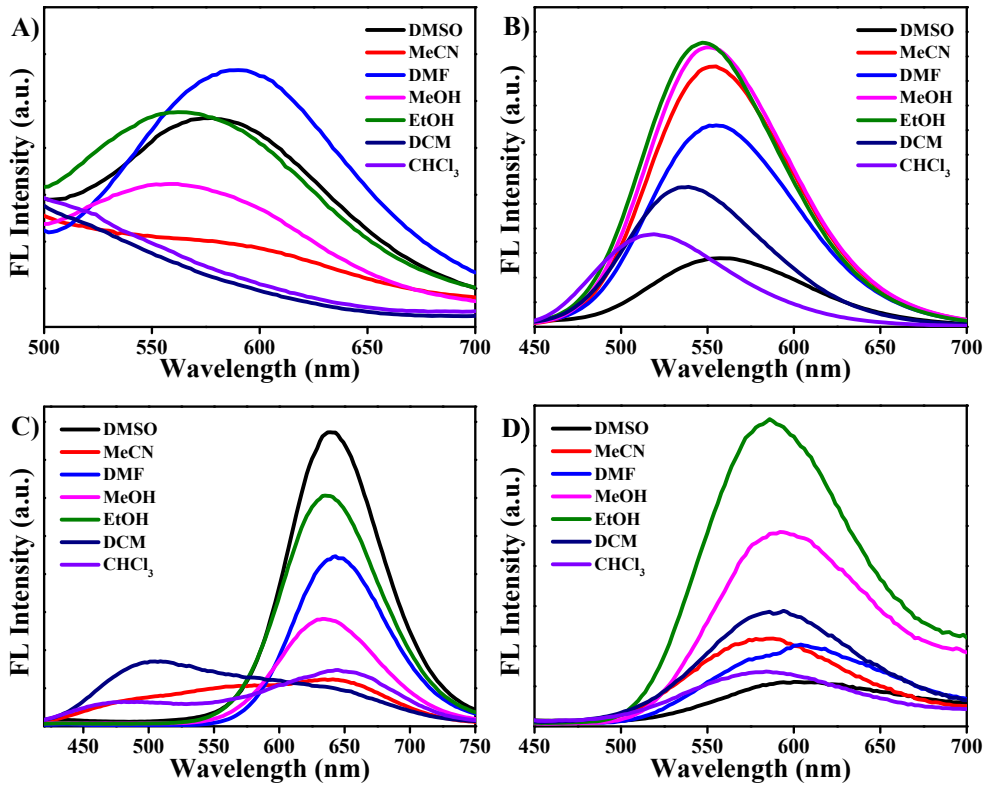

Figure S2. The fluorescence emission spectra of SP-OH dyes in different solvents (c = 10^{-5} mol/L).

A) SP-2-NO_2-Py (λ_{ex} = 410 nm), B) SP-2-NO_2-5-OMe-Py (λ_{ex} = 393 nm), C) SP-5-NO_2-2-OH-Py (λ_{ex} = 385 nm), D) SP-2-NO_2-5-OH-Py (λ_{ex} = 420 nm)

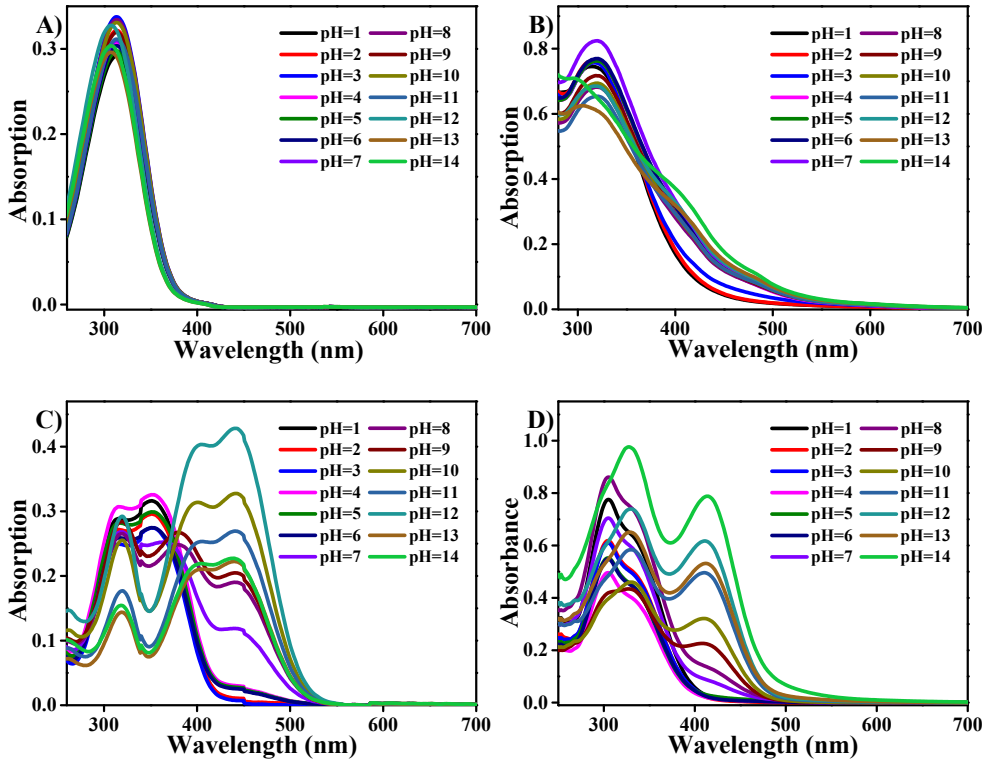

Figure S3. The UV-Vis absorption spectra of SP-OH dyes in different pH (c = 10^{-5} mol/L in water solution).

A) SP-2-NO_2-Py, B) SP-2-NO_2-5-OMe-Py, C) SP-5-NO_2-2-OH-Py, D) SP-2-NO_2-5-OH-Py

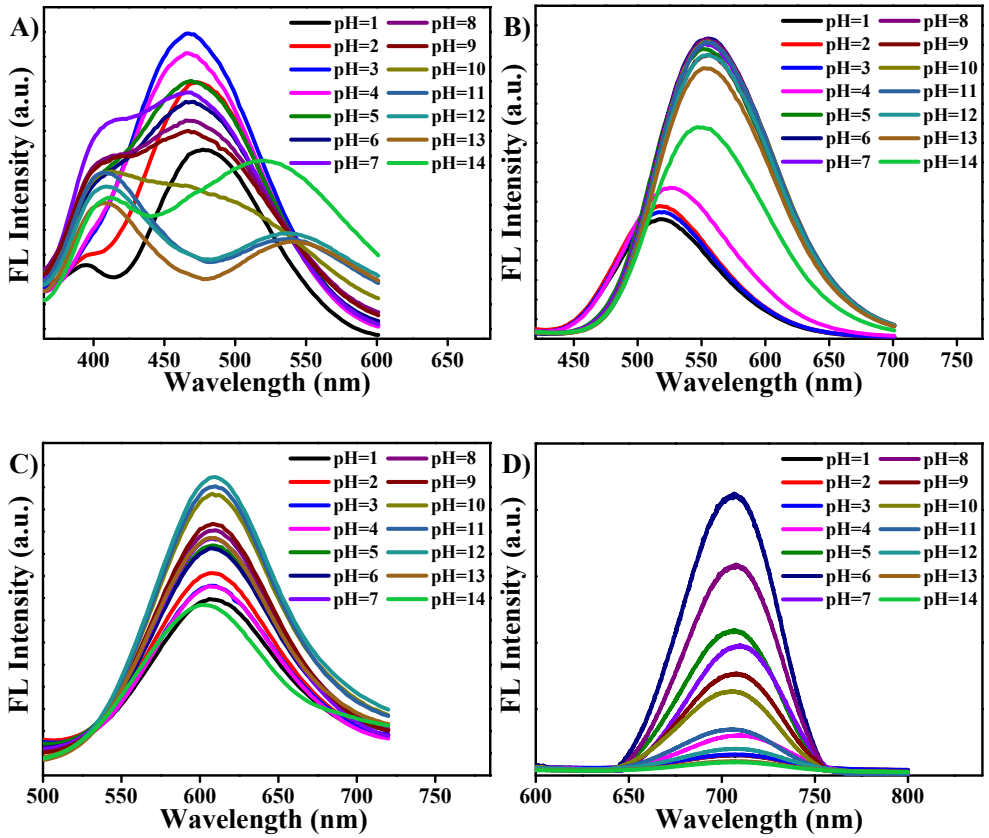

Figure S4. The fluorescence emission spectra of SP-OH dyes in different pH (c = 10^{-5} mol/L in water solution).

A) SP-2-NO_2-Py (λ_{ex} = 345 nm), B) SP-2-NO_2-5-OMe-Py (λ_{ex} = 393 nm), C) SP-5-NO_2-2-OH-Py (λ_{ex} = 380 nm), D) SP-2-NO_2-5-OH-Py (λ_{ex} = 450 nm)

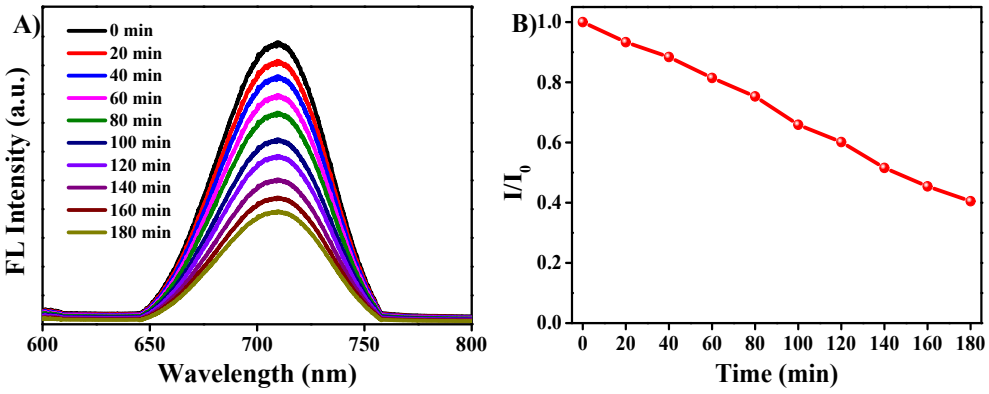

Figure S5. The photostability of SP-2-NO_2-5-OH-Py under continuous illumination at 365 nm (10 W) (c = 10^{-5} M at water solution, λ_{ex}=450 nm)

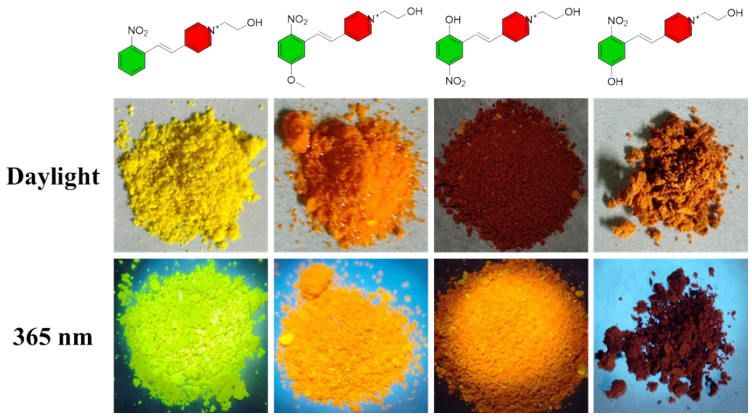

Figure S6. Optical images of SP-OH dyes in solid state under daylight and 365 nm UV irradiation, respectively.

Table S1. Photoluminescent characteristics of SP-2-NO_2-Py in different solvents

Solvent	λ^a_{abs}/nm	λ^a_{em}/nm	Stokes shift/nm	$\varepsilon^b \times 10^4$ (M^{-1}•cm^{-1})	QY[c]/%
DMSO	352	580	228	3.88	2.4
CH_3CN	350	575	225	3.57	1.1
DMF	351	591	240	4.08	2.6
CH_3OH	351	560	209	3.73	1.8
C_2H_5OH	351	563	212	4.80	2.4
CH_2Cl_2	351	*n.d.*	*n.d.*	3.99	*n.d.*
$CHCl_3$	351	*n.d.*	*n.d.*	4.18	*n.d.*

[a] SP-2-NO_2-Py was dissolved in different solvents solution with a concentration of 10^{-5} mol/L. [b] Molar extinction coefficients (ε) were measured at the absorption maximum. [c] Absolute photoluminescence quantum yields (QY) of dyes in DMF solution were determined by using the integrating sphere method. *n.d*: too low to be detected.

Table S2. Photoluminescent characteristics of SP-2-NO_2-5-OMe-Py in different solvents

Solvent	λ^a_{abs}/nm	λ^a_{em}/nm	Stokes shift/nm	$\varepsilon^b \times 10^4$ (M^{-1}•cm^{-1})	QY[c]/%
DMSO	312	558	246	5.83	11.4
CH_3CN	317	553	236	4.86	17.2
DMF	317	555	238	5.64	14.7
CH_3OH	316	551	235	5.36	18.3
C_2H_5OH	316	547	231	5.29	18.5
CH_2Cl_2	319	537	218	5.21	13.6
$CHCl_3$	321	517	196	5.49	12.9

[a] SP-2-NO_2-5-OMe-Py was dissolved in different solvents solution with a concentration of 10^{-5} mol/L. [b] Molar extinction coefficients (ε) were measured at the absorption maximum. [c] Absolute

photoluminescence quantum yields (QY) of dyes in DMF solution were determined by using the integrating sphere method.

Table S3. Photoluminescent characteristics of SP-5-NO_2-2-OH-Py in different solvents

Solvent	λ^a_{abs}/nm	λ^a_{em}/nm	Stokes shift/nm	$\varepsilon^b \times 10^4$ (M^{-1}•cm^{-1})	QY[c]/%
DMSO	321/424/509	640	319/216/131	1.59/1.58/2.52	13.9
CH_3CN	332/413/507	640	308/227/133	1.15/0.86/1.41	6.1
DMF	325/423/513	642	317/219/129	1.09/1.79/3.04	9.2
CH_3OH	328/369/468	634	306/265/166	1.17/1.52/0.38	8.4
C_2H_5OH	329/393/479	635	306/242/156	1.21/1.34/1.67	11.3
CH_2Cl_2	325/377	504/637	179/127/312/260	1.20/1.79	6.7
$CHCl_3$	321/376	479/644	158/103/323/268	1.44/2.02	6.2

[a] SP-5-NO_2-2-OH-Py was dissolved in different solvents solution with a concentration of 10^{-5} mol/L. [b] Molar extinction coefficients (ε) were measured at the absorption maximum. [c] Absolute photoluminescence quantum yields (QY) of dyes in DMF solution were determined by using the integrating sphere method.

Table S4. Photoluminescent characteristics of SP-2-NO_2-5-OH-Py in different solvents

Solvent	λ^a_{abs}/nm	λ^a_{em}/nm	Stokes shift/nm	$\varepsilon^b \times 10^4$ (M^{-1}•cm^{-1})	QY[c]/%
DMSO	306/330/429	601	295/271/172	7.98/6.92/0.81	13.5
CH_3CN	300/325	588	288/263	6.37/5.60	16.5
DMF	304/331/422	605	301/274/183	5.86/5.51/1.35	6.6
CH_3OH	303/325	595	292/270	4.17/3.79	24.1
C_2H_5OH	301/324	587	286/263	6.22/5.50	29.7
CH_2Cl_2	310/329	592	282/263	2.88/2.80	4.9
$CHCl_3$	310/333	583	273/250	6.27/5.94	5.3

[a] SP-2-NO_2-5-OH-Py was dissolved in different solvents solution with a concentration of 10^{-5} mol/L. [b] Molar extinction coefficients (ε) were measured at the absorption maximum. [c] Absolute photoluminescence quantum yields (QY) of dyes in DMF solution were determined by using the integrating sphere method.

Table S5. Photoluminescent characteristics of SP-2-NO_2-Py in different pH

pH	λ^a_{abs}/nm	λ^a_{em}/nm	Stokes shift/nm	$\varepsilon^b \times 10^4$ (M^{-1}•cm^{-1})	QY[c]/%
1	313	477	164	2.92	0.53
2	313	473	160	3.22	0.89
3	313	466	153	3.38	1.07
4	313	466	153	3.07	0.98
5	313	403/466	90/153	2.98	0.86
6	313	403/466	90/153	3.04	0.81
7	313	414/468	101/155	3.09	0.80
8	313	414/468	101/155	3.35	0.74
9	313	414/468	101/155	3.19	0.74
10	313	412/499	99/186	3.31	0.65
11	313	408/537	95/224	3.12	0.58
12	307	408/538	101/231	3.28	0.59
13	307	408/540	101/233	2.96	0.61
14	307	412/520	105/213	3.04	0.64

[a] SP-2-NO_2-Py was dissolved in different pH aqueous solution with a concentration of 10^{-5} mol/L. [b] Molar extinction coefficients (ε) were measured at the absorption maximum. [c] Absolute photoluminescence quantum yields (QY) of dyes in DMF solution were determined by using the integrating sphere method.

Table S6. Photoluminescent characteristics of SP-2-NO_2-5-OMe-Py in different pH

pH	λ^a_{abs}/nm	λ^a_{em}/nm	Stokes shift/nm	$\varepsilon^b \times 10^4$ (M^{-1}•cm^{-1})	QY[c]/%
1	315	518	203	7.46	2.5
2	316	518	202	7.64	2.4
3	317	518	201	7.58	2.5
4	317	525	208	7.64	2.7
5	319	552	233	7.63	4.2
6	319	555	236	7.70	4.3
7	319	553	234	8.29	4.3
8	319	555	236	6.83	4.4
9	320	555	235	7.18	3.9
10	320	555	235	6.95	4.3
11	320	555	235	6.55	4.4
12	319	555	236	6.86	4.0
13	306	555	249	6.26	3.7
14	295	548	253	7.11	3.2

[a] SP-2-NO_2-5-OMe-Py was dissolved in different pH aqueous solution with a concentration of 10^{-5} mol/L. [b] Molar extinction coefficients (ε) were measured at the absorption maximum. [c] Absolute photoluminescence quantum yields (QY) of dyes in DMF solution were determined by using the integrating sphere method.

Table S7. Photoluminescent characteristics of SP-5-NO_2-2-OH-Py in different pH

pH	λ^a_{abs}/nm	λ^a_{em}/nm	Stokes shift/nm	$\varepsilon^b \times 10^4$ (M^{-1}•cm^{-1})	QY[c]/%
1	316/351	607	291/256	2.91/3.17	3.8
2	315/351	607	292/256	2.73/2.98	4.1
3	315/352	607	292/255	2.52/2.77	3.9
4	316/352/441	607	291/255/166	3.09/3.28/0.32	4.2
5	316/351/441	608	292/257/167	2.84/3.02/0.29	4.5
6	316/352/441	608	292/256/167	2.61/2.77/0.27	4.3
7	319/366/441	608	289/242/167	2.70/2.53/1.21	4.4
8	319/379/441	608	289/229/167	2.69/2.51/1.92	4.5
9	319/380/442	608	289/228/166	2.86/2.69/2.08	4.5
10	319/400/441	608	289/208/167	2.58/3.16/3.29	4.8
11	319/405/441	608	289/203/167	1.79/2.57/2.72	4.7
12	319/405/441	608	289/203/167	2.94/4.05/4.31	4.9
13	319/405/441	608	289/203/167	1.46/2.12/2.25	4.4
14	318/404/438	603	285/199/165	1.57/2.21/2.29	4.1

[a] SP-5-NO_2-2-OH-Py was dissolved in different pH aqueous solution with a concentration of 10^{-5} mol/L. [b] Molar extinction coefficients (ε) were measured at the absorption maximum. [c] Absolute photoluminescence quantum yields (QY) of dyes in DMF solution were determined by using the integrating sphere method.

Table S8. Photoluminescent characteristics of SP-2-NO_2-5-OH-Py in different pH

pH	λ^a_{abs}/nm	λ^a_{em}/nm	Stokes shift/nm	$\varepsilon^b \times 10^4$ (M^{-1}•cm^{-1})	QY[c]/%
1	305	707	402	7.79	0.4
2	305	707	402	6.22	0.3
3	305	707	402	6.15	0.4
4	305	709	404	4.99	1.1
5	305	707	402	5.56	2.1
6	305	707	402	5.52	3.7
7	305	709	404	7.06	1.9
8	305	708	403	8.66	3.2
9	308/327/411	707	399/380/296	4.28/4.38/2.31	1.5
10	331/411	706	375/295	4.64/3.25	1.7
11	331/411	706	375/295	5.88/5.01	1.3
12	331/411	707	376/296	7.42/6.21	0.8
13	329/411	707	378/296	6.57/5.37	0.3
14	329/414	706	377/292	9.83/7.93	0.2

[a] SP-2-NO_2-5-OH-Py was dissolved in different pH aqueous solution with a concentration of 10^{-5} mol/L. [b] Molar extinction coefficients (ε) were measured at the absorption maximum. [c] Absolute photoluminescence quantum yields (QY) of dyes in DMF solution were determined by using the integrating sphere method.

3. Density functional theory (DFT) calculations

The ground state structures of all SP-OH dyes were optimized by using B3LYP/6-311+G (d, p) level. The time-dependent density functional theory (TD-DFT) calculation used the B3LYP/6-311+G (d, p) method based on their optimized S_0 geometries. All the calculations were performed in Gaussian 09. The natural transition orbitals were analyzed using Multiwfn 3.8[1-4].

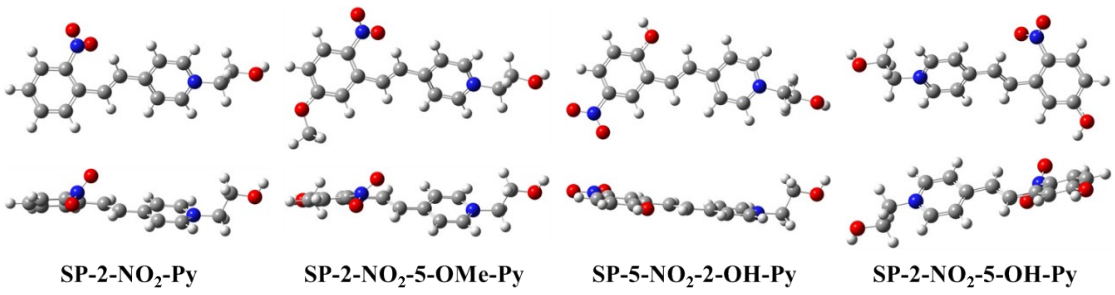

Figure S7. Ground-state molecular configurations of the optimized SP-OH dyes at different angles

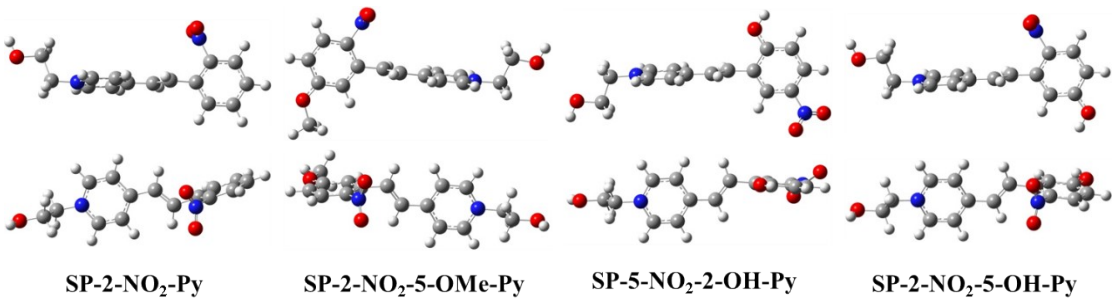

Figure S8. Excited-state molecular configurations of the optimized SP-OH dyes at different angles

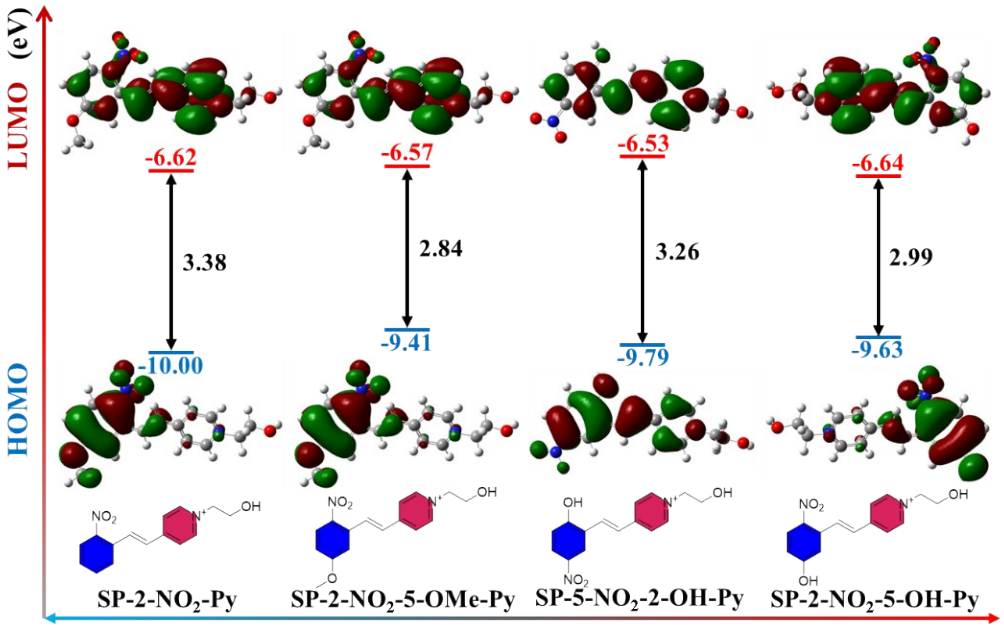

Figure S9. Ground-state HOMO-LUMO energy levels and molecular orbitals of SP-OH dyes

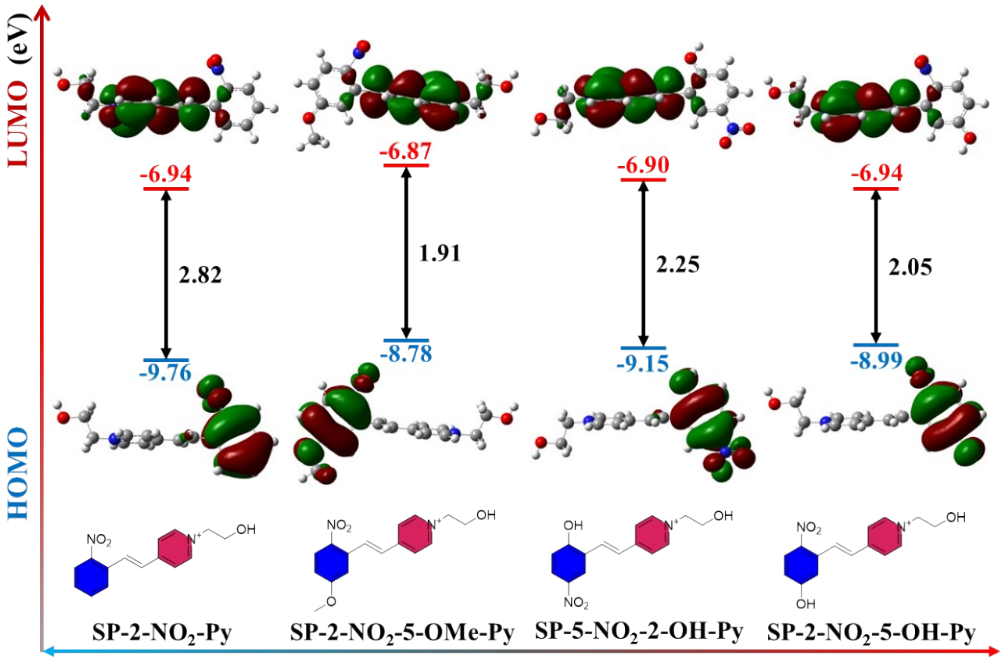

Figure S10. Excited-state HOMO-LUMO energy levels and molecular orbitals of SP-OH dyes

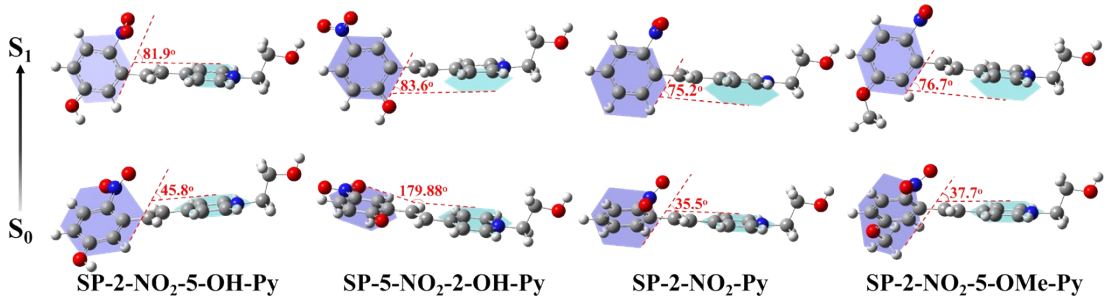

Figure S11. The molecular geometries and dihedral angle of SP-OH dyes in the ground state (S_0) and the excited state (S_1)

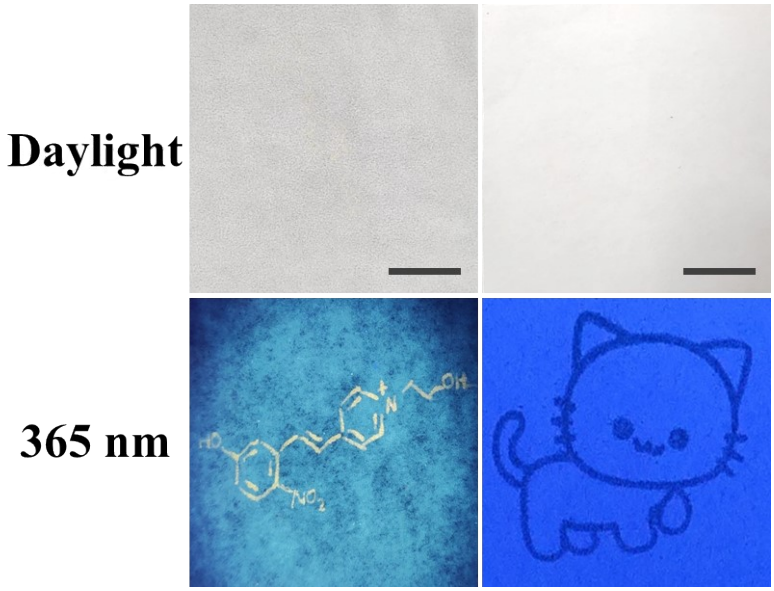

Fig. S12. Typical optical images of the SP-2-NO_2-5-OH-Py dye anti-counterfeiting pattern drawn on weighing paper (Left) and printing paper (Right). Scale bar: 0.5 cm.

4. Syntheses and characterization

4.1 *Synthesis of compound 1-(2-Hydroxyethyl)-4-methylpyridin-1-ium bromide*

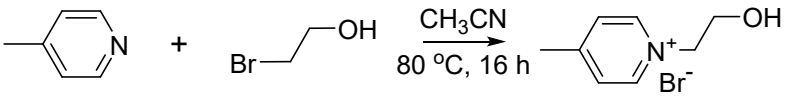

Scheme S1. Synthesis route of compound 1-(2-Hydroxyethyl)-4-methylpyridin-1-ium bromide

4-methylpyridine (0.465 g, 5 mmol) and 2-bromoethanol (0.625 g, 5 mmol) were dissolved in anhydrous acetonitrile (50 mL). The reaction mixture was heated at 80 °C under reflux for 16 h. After the reaction was completed and returned to room temperature. The solvent was removed by reducing pressure concentration to afford the product as a pale-yellow oil (1.063 g, 92.37% yield), which was used directly in the next reaction without further purification. **^{1}H NMR** (400 MHz, DMSO-d_6): δ(ppm) 2.54 (s, 3H), 3.76 (t, *J*=8 Hz, 2H), 4.63 (t, *J*=12 Hz, 2H), 5.16 (s, 1H), 7.95 (d, *J*=8 Hz, 2H), 8.90 (d, *J*=8 Hz, 2H). **^{13}C NMR** (100 MHz, DMSO-d_6): δ(ppm) 21.87, 48.94, 60.39, 62.43, 128.35, 144.51, 159.18.

4.2 *General procedure for the synthesis of SP-OH dyes*

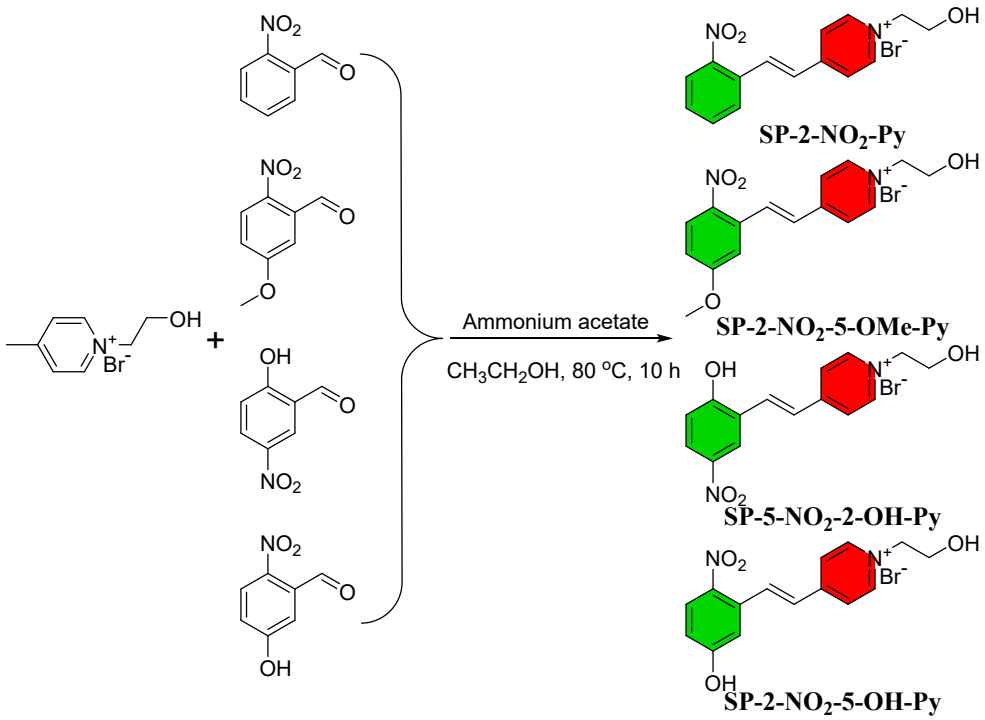

Scheme S2. Synthesis route of SP-OH dyes through the Knoevenagel reaction

1-(2-Hydroxyethyl)-4-methylpyridin-1-ium bromide (1.0 equiv) and 2-Nitrobenzaldehyde derivatives or 5-Nitrosalicylaldehyde (1.0 equiv) were added in a sufficient volume of anhydrous ethanol to fully dissolve the reactants. The reaction mixture was heated under an argon atmosphere at 80 °C for 10 min. Ammonium acetate (0.05 equiv) was then added in one portion. The resulting mixture was maintained under argon at 80 °C and stirred for a further 10 h until complete consumption of the starting material was observed by TLC. After the reaction was completed, the ambient temperature was restored. Then the excess ethanol was removed by reducing pressure concentration, and the crude product was further purified by silica gel column chromatography (Dichloromethane: Methanol=20:1~10:1, v/v).

Compound **SP-2-NO$_2$-Py** was obtained as orange-yellow solid (71.25 mg, 20.34%). **^{1}H NMR** (400 MHz, DMSO-d_6): δ(ppm) 3.83 (t, *J*=12 Hz, 2H), 4.59 (t, *J*=8 Hz, 2H), 6.85 (t, *J*=16 Hz, 1H), 7.00 (d, *J*=8 Hz, 1H), 7.24 (t, *J*=16 Hz, 1H), 7.52 (d, *J*=16 Hz, 1H), 7.66 (d, *J*=8 Hz, 1H), 8.04 (d, *J*=20 Hz, 1H), 8.21 (d, *J*=8 Hz, 2H), 8.85 (d, *J*=8 Hz, 2H). **^{13}C NMR** (100 MHz, DMSO-d_6): δ(ppm) 21.87, 60.52, 62.26, 116.95, 119.89, 122.38, 123.22, 123.64, 128.40, 129.32, 132.17, 137.12, 144.92, 154.03, 157.56. HRMS: calculated for $C_{15}H_{15}N_2O_3Br$ $[M+H]^+$: 352.02, found 352.04.

Compound **SP-2-NO$_2$-5-OMe-Py** was obtained as orange solid (38.53 mg, 12.82%).

^{1}H NMR (400 MHz, DMSO-d_6): δ(ppm) 3.74 (t, *J*=60 Hz, 5H), 4.55 (d, *J*=12 Hz, 2H), 6.86 (t, *J*=16 Hz, 1H), 7.02 (d, *J*=8 Hz, 1H), 7.30 (d, *J*=8 Hz, 1H), 7.49 (d, *J*=16 Hz, 1H), 8.08 (d, *J*=16 Hz, 1H), 8.23 (d, *J*=8 Hz, 2H), 8.85 (d, *J*=4 Hz, 2H). **^{13}C NMR** (100 MHz, DMSO-d_6): δ(ppm) 56.53, 60.53, 62.35, 113.93, 119.75, 120.24, 122.63, 123.52, 123.76, 136.57, 145.01, 146.65, 148.56, 153.83. HRMS: calculated for $C_{16}H_{17}N_2O_4Br$ $[M+H]^+$: 382.03, found 380.24.

Compound **SP-5-NO_2-2-OH-Py** was obtained as bright-red solid (261.55 mg, 71.23%). **^{1}H NMR** (400 MHz, DMSO-d_6): δ(ppm) 3.84 (t, *J*=8 Hz, 2H), 4.57 (t, *J*=8 Hz, 2H), 7.08 (d, *J*=8 Hz, 1H), 7.39 (d, *J*=16 Hz, 1H), 7.60 (d, *J*=8 Hz, 1H), 7.96 (m, 2H), 8.18 (d, *J*=8 Hz, 2H), 8.87 (d, *J*=8 Hz, 2H). **^{13}C NMR** (100 MHz, DMSO-d_6): δ(ppm) 60.48, 62.50, 117.35, 122.97, 124.21, 125.36, 126.13, 127.15, 134.77, 140.32, 145.23, 153.31, 163.07. HRMS: calculated for $C_{15}H_{15}N_2O_4Br$ $[M+H]^+$: 368.02, found 366.00.

Compound **SP-2-NO_2-5-OH-Py** was obtained as dark orange solid (213.89 mg, 58.25%). **^{1}H NMR** (400 MHz, DMSO-d_6): δ(ppm) 3.83 (t, *J*=8 Hz, 2H), 4.56 (t, *J*=8 Hz, 2H), 6.71 (t, *J*=16 Hz, 1H), 6.87 (d, *J*=8 Hz, 1H), 7.15 (d, *J*=8 Hz, 1H), 7.44 (d, *J*=16 Hz, 1H), 8.07 (d, *J*=16 Hz, 1H), 8.20 (d, *J*=8 Hz, 2H), 8.82 (d, *J*=4 Hz, 2H). **^{13}C NMR** (100 MHz, DMSO-d_6): δ(ppm) 60.53, 62.77, 115.80, 117.31, 124.67, 127.46, 128.46, 134.53, 137.54, 140.15, 145.55, 152.57, 163.09. HRMS: calculated for $C_{15}H_{15}N_2O_4Br$ $[M+H]^+$: 368.02, found 366.28.

5. Supplemental Spectra

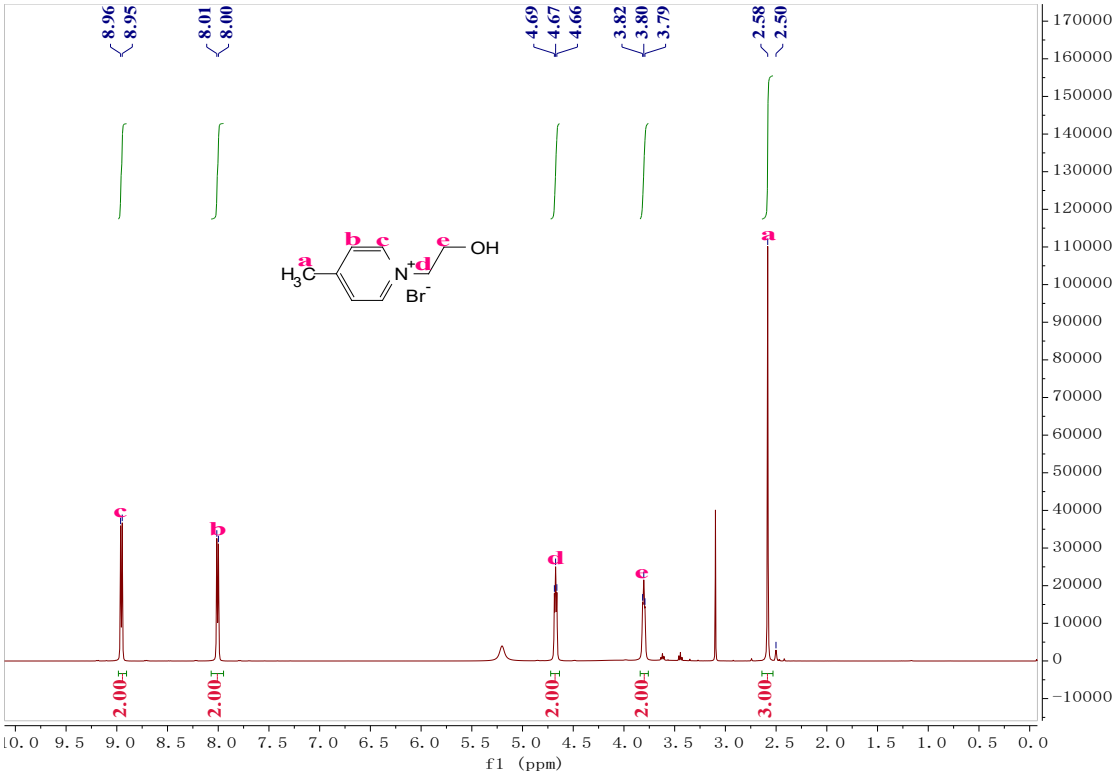

Fig. S13. [1]H NMR spectrum of 1-(2-Hydroxyethyl)-4-methylpyridin-1-ium bromide

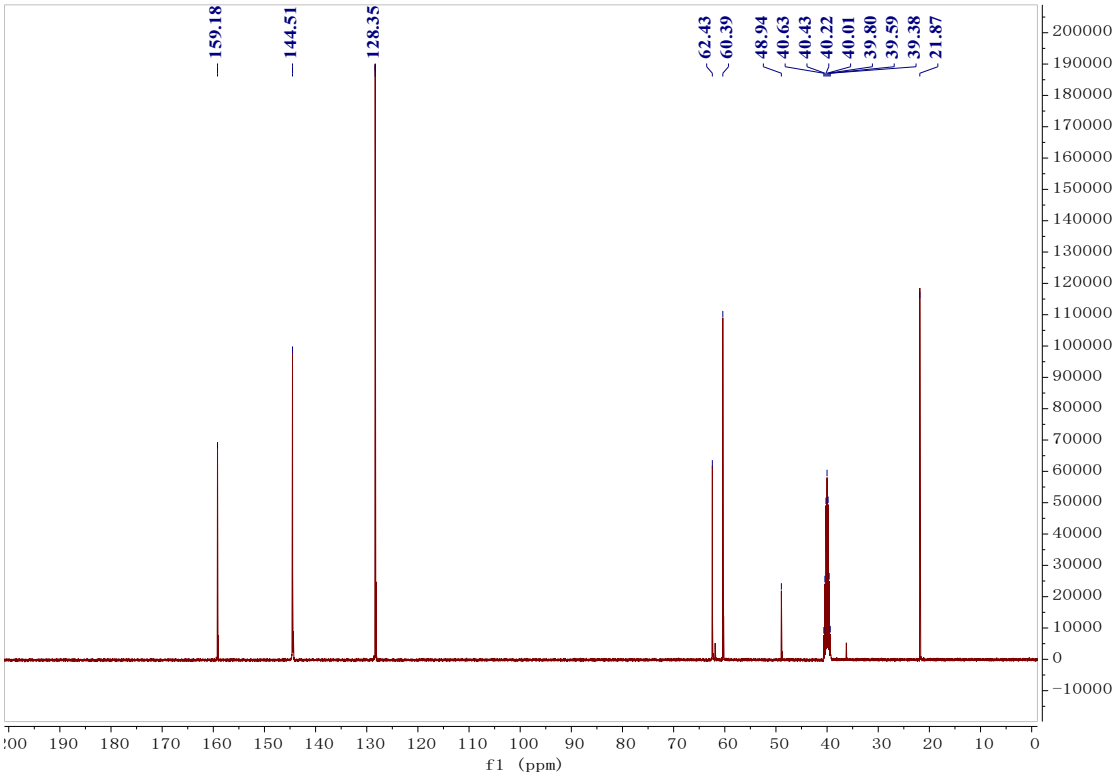

Fig. S14. [13]C NMR spectrum of 1-(2-Hydroxyethyl)-4-methylpyridin-1-ium bromide

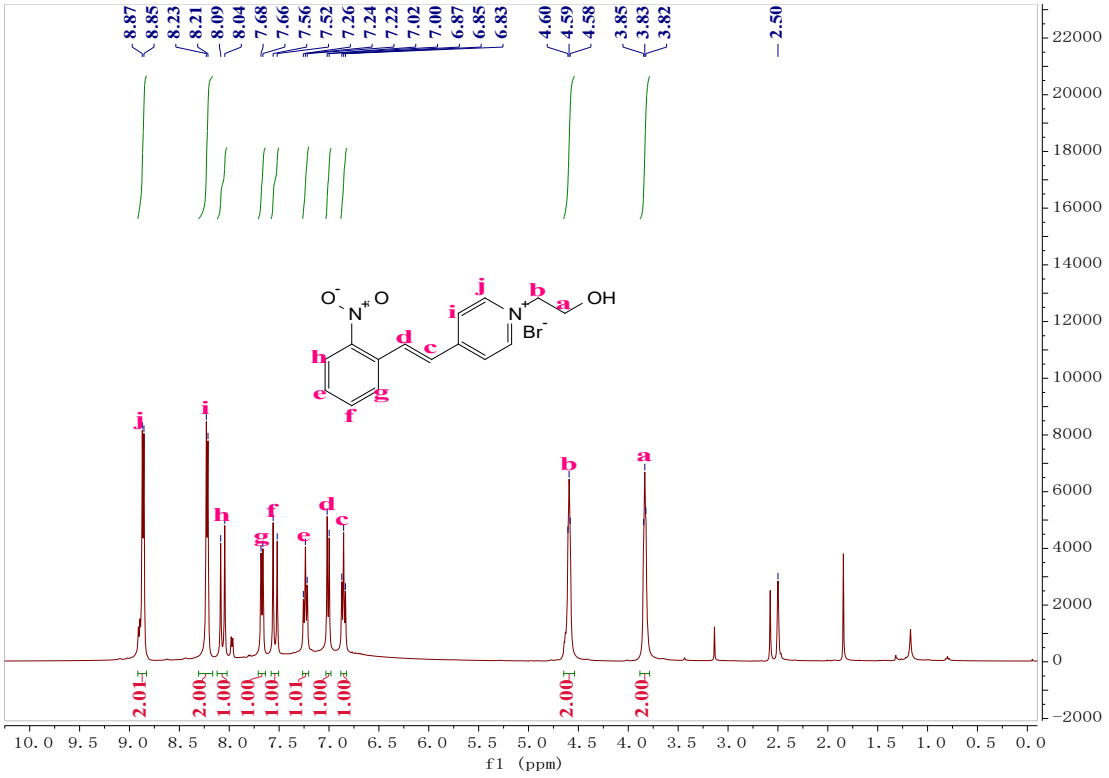

Fig. S15. [1]H NMR spectrum of compound **SP-2-NO$_2$-Py**

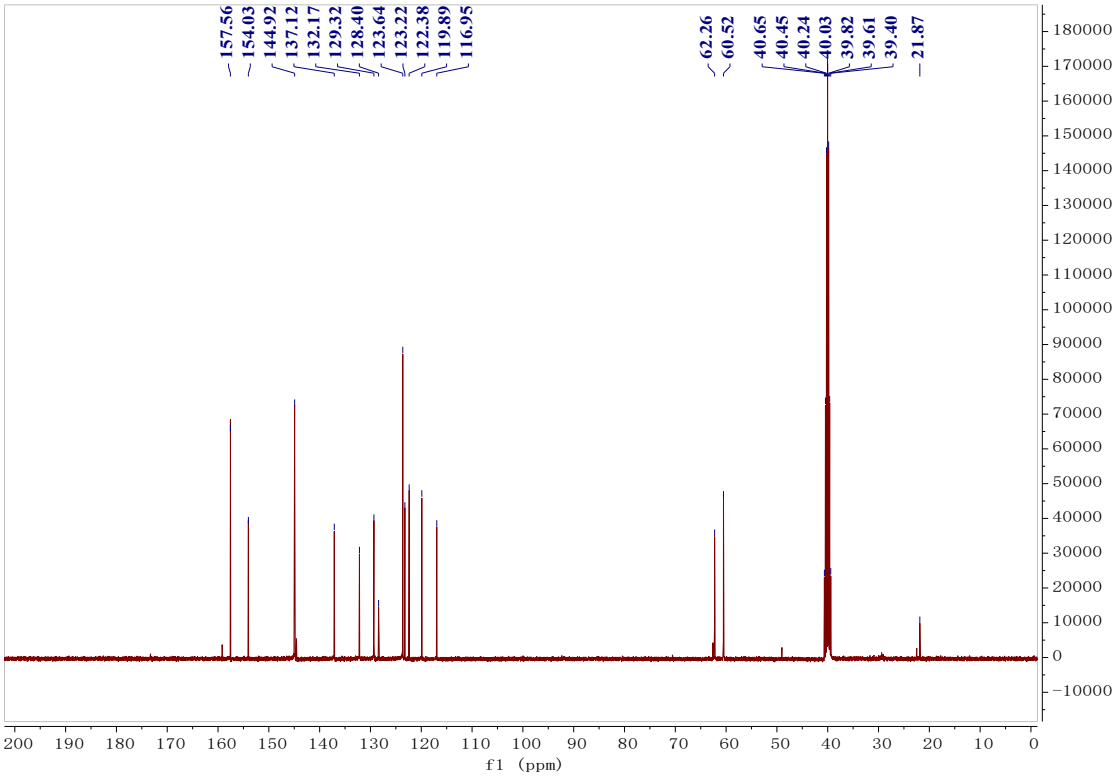

Fig. S16. [13]C NMR spectrum of compound **SP-2-NO$_2$-Py**

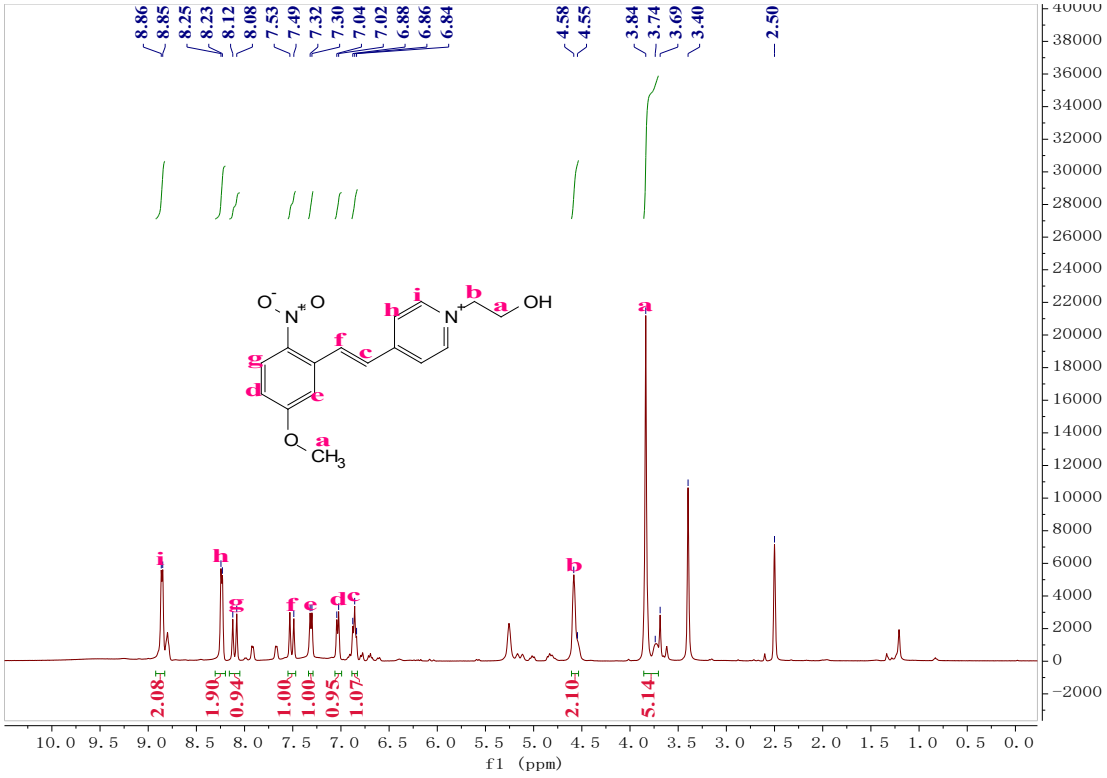

Fig. S17. ^{1}H NMR spectrum of compound **SP-2-NO$_2$-5-OMe-Py**

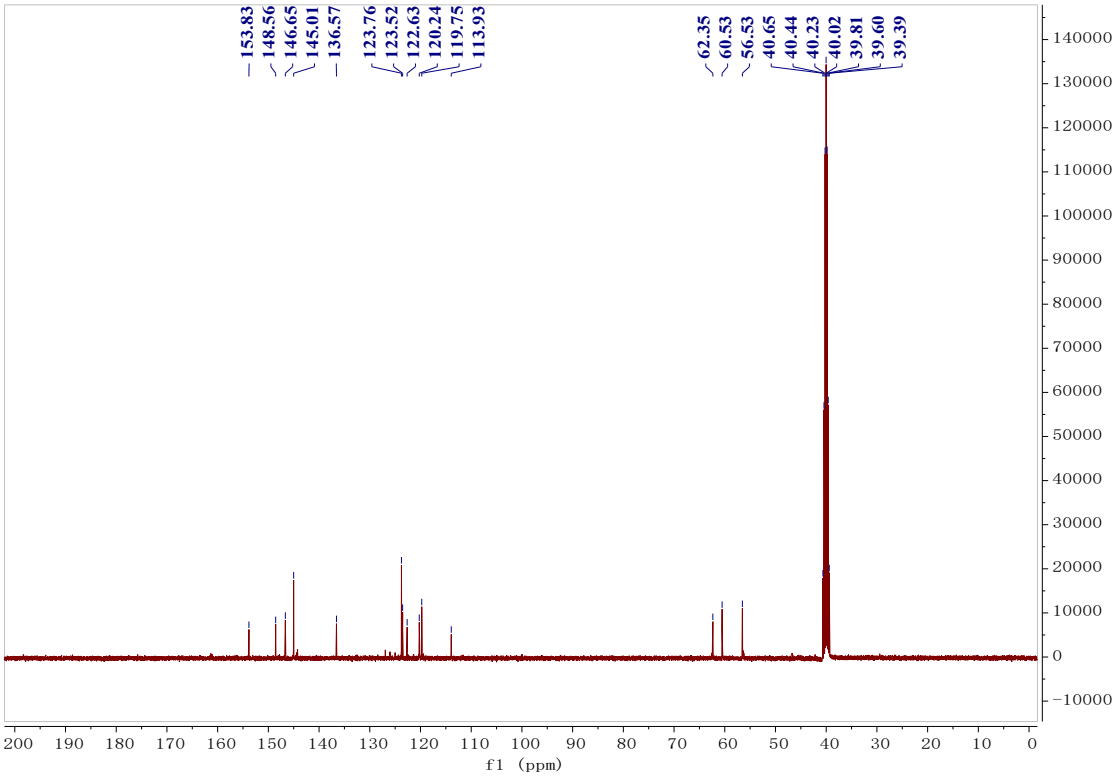

Fig. S18. ^{13}C NMR spectrum of compound **SP-2-NO$_2$-5-OMe-Py**

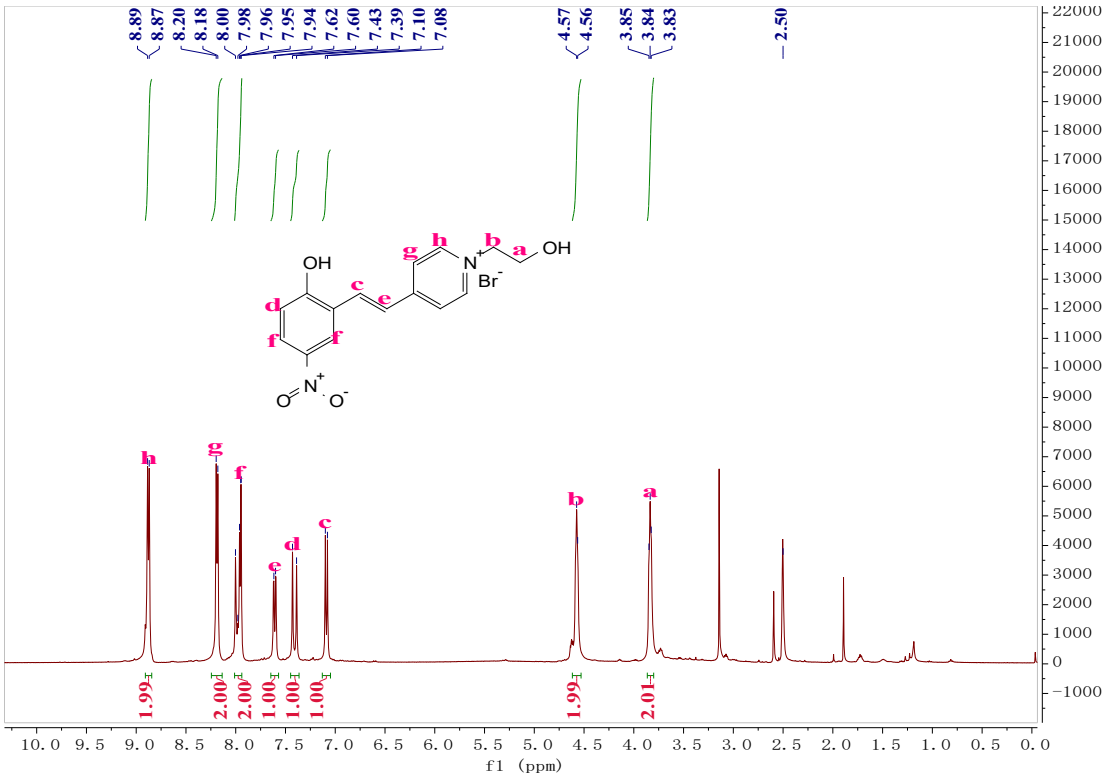

Fig. S19. ^{1}H NMR spectrum of compound **SP-5-NO$_2$-2-OH-Py**

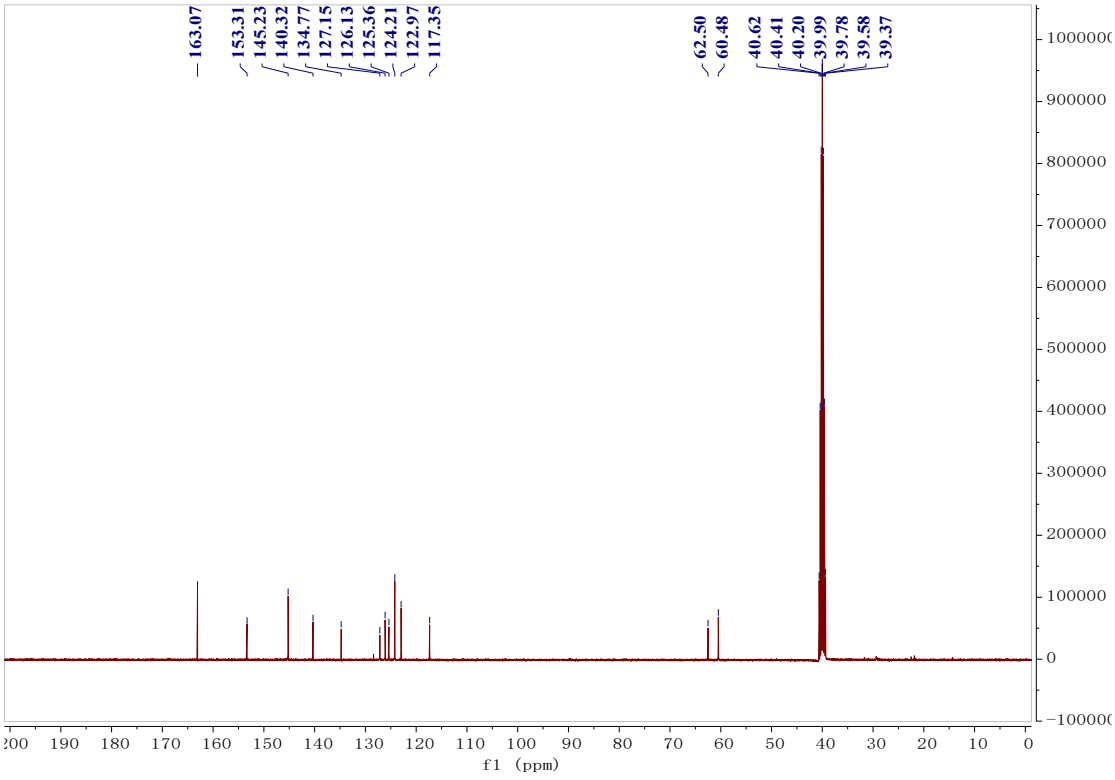

Fig. S20. ^{13}C NMR spectrum of compound **SP-5-NO$_2$-2-OH-Py**

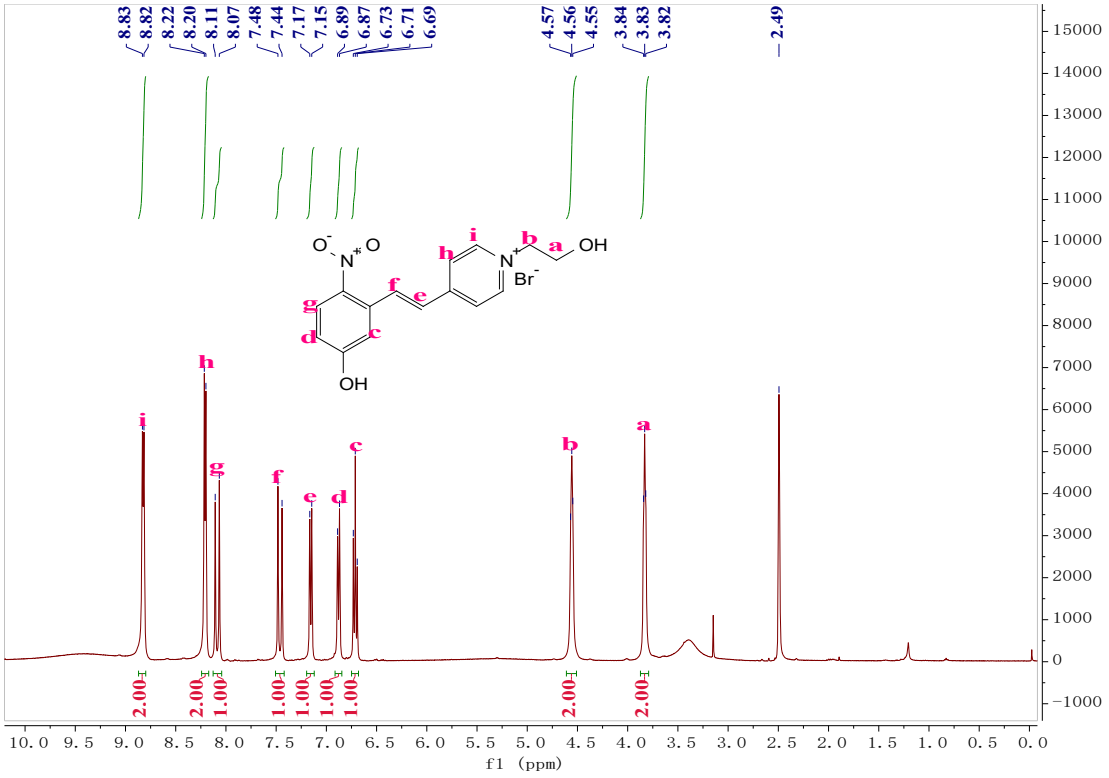

Fig. S21. ^{1}H NMR spectrum of compound **SP-2-NO$_2$-5-OH-Py**

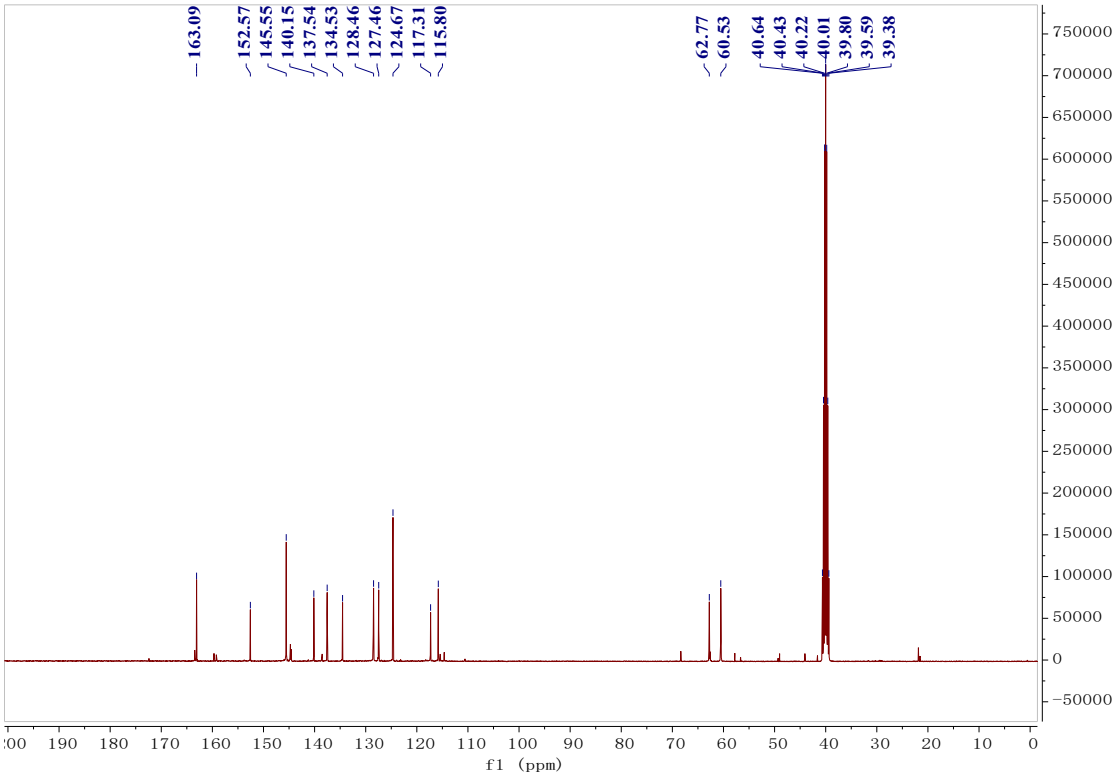

Fig. S22. ^{13}C NMR spectrum of compound **SP-2-NO$_2$-5-OH-Py**

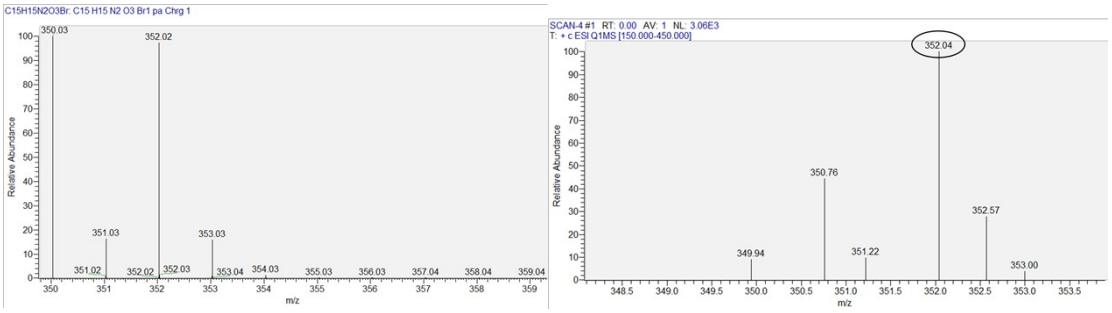

Fig. S23. The high-resolution mass spectrometry of **SP-2-NO_2-Py**

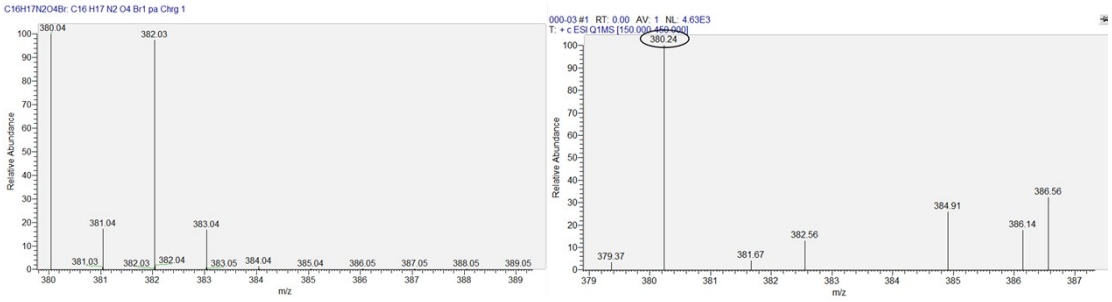

Fig. S24. The high-resolution mass spectrometry of **SP-2-NO_2-5-OMe-Py**

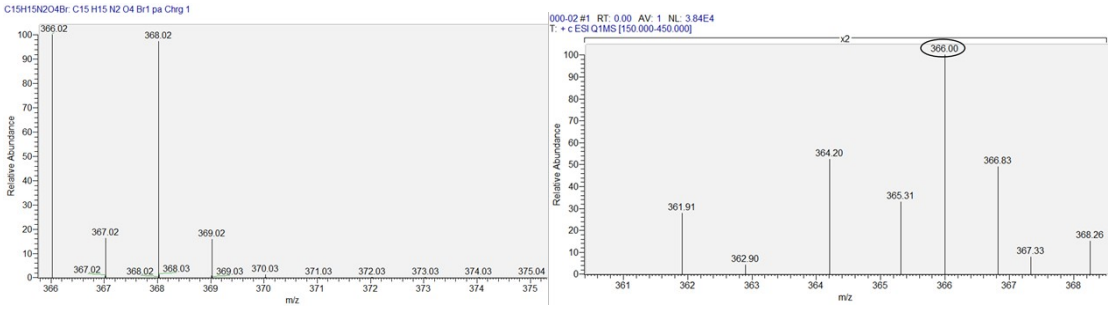

Fig. S25. The high-resolution mass spectrometry of **SP-5-NO_2-2-OH-Py**

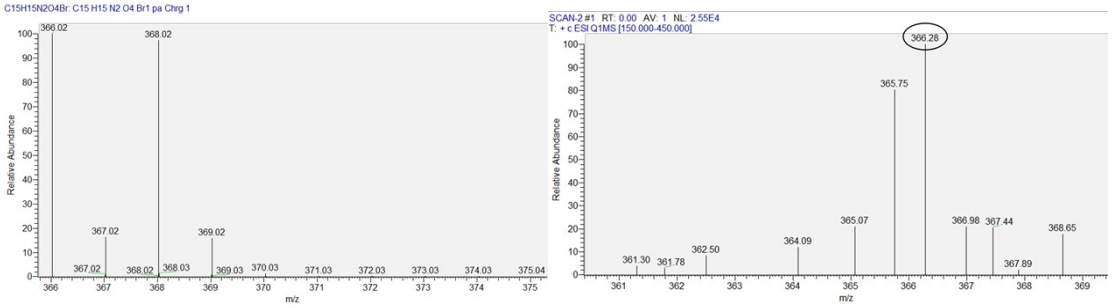

Fig. S26. The high-resolution mass spectrometry of **SP-2-NO_2-5-OH-Py**

6. References

[1] Tian Lu, Fei-Wu Chen. Multiwfn: A multifunctional wavefunction analyzer. Journal of Computational Chemistry, 2012, **33**, 580-592.

[2] Tian Lu. A comprehensive electron wavefunction analysis toolbox for chemists, Multiwfn. The Journal of Chemical Physics, 2024, **161**, 082503.

[3] Saeedreza Emamian, Tian Lu, Holger Kruse, Hamidreza Emamian. Exploring nature and predicting strength of hydrogen bond: A correlation analysis between atoms-in-molecules descriptors, binding energies, and energy components of symmetry-adapted perturbation theory. Journal of Computational Chemistry, 2019, **40**, 2868-2881.

[4] Tian Lu, Qin-Xue Chen. Independent gradient model based on Hirshfeld partition: A new method for visual study of interactions in chemical systems. Journal of Computational Chemistry, 2022, **43**, 539-555.